Enhanced Nitrate Fraction

Liu, Y. C.; Wu, Z. J.; Qiu, Y. T.; Tian, P.; Liu, Q.; Chen, Y.; Song, M.; Hu, M.

DOI:
10.1029/2023gl105505

Geophysical Research Letters

RESEARCH LETTER
10.1029/2023GL105505

Key Points:

- Particles with more inorganic compounds, particularly nitrate, can exist in a liquid state at lower relative humidity levels
- Particles with normalized aerosol liquid water content larger than 0.3 exist in a liquid state
- Nitrate-dominated particles can serve as key seeds where secondary aerosol formation can occur via multiphase reactions

Supporting Information:

Supporting Information may be found in the online version of this article.

Correspondence to:
Z. J. Wu,
zhijunwu@pku.edu.cn

Citation:
Liu, Y. C., Wu, Z. J., Qiu, Y. T., Tian, P., Liu, Q., Chen, Y., et al. (2023). Enhanced nitrate fraction: Enabling urban aerosol particles to remain in a liquid state at reduced relative humidity. *Geophysical Research Letters*, *50*, e2023GL105505. https://doi.org/10.1029/2023GL105505

Received 27 JUL 2023
Accepted 13 OCT 2023

Author Contributions:
Conceptualization: Y. C. Liu, Z. J. Wu
Data curation: Y. C. Liu
Formal analysis: Y. C. Liu, Y. Chen
Investigation: Y. C. Liu, Z. J. Wu, Y. T. Qiu, M. Song, M. Hu
Methodology: Y. C. Liu, Z. J. Wu, Y. T. Qiu, P. Tian, Q. Liu
Supervision: Y. C. Liu, M. Hu
Visualization: Y. C. Liu
Writing – original draft: Y. C. Liu
Writing – review & editing: Y. C. Liu, Y. Chen, M. Song

Enhanced Nitrate Fraction: Enabling Urban Aerosol Particles to Remain in a Liquid State at Reduced Relative Humidity

Y. C. Liu[1], Z. J. Wu[1,2], Y. T. Qiu[1], P. Tian[3], Q. Liu[4], Y. Chen[5], M. Song[6], and M. Hu[1]

[1]State Key Joint Laboratory of Environmental Simulation and Pollution Control, College of Environmental Sciences and Engineering, Peking University, Beijing, China, [2]Collaborative Innovation Center of Atmospheric Environment and Equipment Technology, Nanjing University of Information Science and Technology, Nanjing, China, [3]Beijing Weather Modification Center, Beijing, China, [4]State Key Laboratory of Severe Weather & Key Laboratory of Atmospheric Chemistry of CMA, Chinese Academy of Meteorological Sciences, Beijing, China, [5]School of Geography, Earth and Environmental Sciences, University of Birmingham, Birmingham, UK, [6]Department of Earth and Environmental Sciences, Jeonbuk National University, Jeonju, Republic of Korea

Abstract Nitrate has become the primary inorganic compound in urban aerosol particles, but its effects on particle phase state, which is crucial in multiphase chemistry, remains largely unknown. Herein, particle rebound measurements were conducted to explore the relationship between the liquid–phase–transition threshold relative humidity ($RH_{threshold}$) and the inorganic compounds mass fraction in dry particles (F_{inorg}). Results revealed negative correlations between $RH_{threshold}$ and F_{inorg}, with more nitrate leading to lower $RH_{threshold}$. Even with RH < 20%, particles with ~50% nitrate mass fraction remained in non-solid state. Taking Beijing as an example, decreases were observed in $RH_{threshold}$ from 64% in 2015 to below 53% nowadays during the moderate-pollution periods ($PM_{2.5}$ = 35–75 μg/m^3) due to an enhanced nitrate fraction. This allowed urban aerosol particles to exist in liquid state at lower RH, and consequently, kinetic limitation by bulk diffusion in nitrate-dominated particles might be negligible, making them key seeds for secondary aerosol formation through multiphase reactions.

Plain Language Summary The phase state of aerosol particles plays a crucial role in the mass-transfer processes between gas and particles, which is essential for determining particle mass concentration. Investigating the characteristics of the aerosol phase state is crucial for comprehending the mechanisms behind secondary particle formation and improving air quality. Currently, the chemical composition of urban aerosol particles has shown notable changes. The mass fraction of inorganic components has increased, with nitrate emerging as the dominant inorganic component. However, the impacts of these changes on the phase state of urban aerosol particles remain largely unknown. This study demonstrates that particles with a higher mass fraction of inorganic compounds, particularly nitrate, tend to exist in a liquid state. Consequently, an increased nitrate fraction allows urban aerosol particles to exist in a liquid state at lower relative humidity levels. These findings suggest that changes in the phase state of particles due to changes in chemical properties in urban aerosol particles should be considered to accurately gauge the mass-transfer processes and promote the air quality improvements in urban cities.

1. Introduction

Atmospheric particles play a profound role in air quality, global climate, and human health (Pöschl, 2005). These effects are closely related to the physical and chemical properties of particles, with the phase state of particles being critical. Numerous studies have confirmed that the phase state of particles plays a crucial role in determining the mass transfer between gas and particles (Davies & Wilson, 2015; Shiraiwa et al., 2010, 2011), thereby influencing various chemical and physical processes in the atmosphere, including gas–particle partitioning (Pöschl, 2005), multiphase reactions (Kuwata & Martin, 2012; Shiraiwa et al., 2011), and the chemical lifetime of air pollutants like polycyclic aromatic hydrocarbons (Mu et al., 2018). Therefore, it is essential to understand the phase state of particles in the atmosphere to accurately assess the impacts of aerosol particles on air quality and climate.

Over the past few decades, several studies have focused on the phase state of secondary organic aerosol particles (SOA) (Reid et al., 2018). It is well established that, under specific environmental conditions, the glass transition temperature of SOA, which represents the phase state, increases with the molecular weight of its compounds and varies based on the atomic oxygen-to-carbon ratio (Kaluarachchi et al., 2022; Koop et al., 2011; Kucinski et al., 2019; Lilek & Zuend, 2022; Reid et al., 2018; Rothfuss & Petters, 2017; Shiraiwa et al., 2017; Song et al., 2021). Additionally, the functional groups (Grayson et al., 2017; Reid et al., 2018) and the volatile organic compounds and oxidants used to generate SOA can influence their phase state (Bateman, Bertram, & Martin, 2015; Pajunoja et al., 2014; Saukko et al., 2012; Song et al., 2015, 2016). Aerosol liquid water content (ALWC), which varies with ambient relative humidity (RH) and temperature, also strongly affects the phase state of SOA (Bateman, Bertram, & Martin, 2015; Hosny et al., 2016; Renbaum-Wolff et al., 2013; Saukko et al., 2012). With increasing ALWC, the viscosity of SOA, which is an indicator of the phase state, decreases due to the plasticizing effect of water, (Koop et al., 2011). Consequently, semi-empirical methods have been developed to predict the glass transition temperature of SOA (DeRieux et al., 2018; Li et al., 2020; Shiraiwa et al., 2017).

In contrast to SOA, there have been limited studies on the phase state of inorganic–organic mixed particles. Laboratory experiments have shown that an increased mass fraction of inorganic particles significantly decreases the viscosity of inorganic–organic mixtures at a given RH (Bateman, Bertram, & Martin, 2015; Power et al., 2013; Song et al., 2021; Tong et al., 2022). Model simulations have revealed that the viscosity of sucrose–$NaNO_3$ mixed particles with an organic-to-inorganic dry mass ratio (OIR) of 3:2 is one order of magnitude lower than that with an OIR of 4:1 at RH = 40% (Lilek & Zuend, 2022). Previous field observations have suggested that, under the influence of a high mass fraction of inorganic compounds, particles in the atmosphere of Beijing transition into a liquid state when RH exceeds 60% (Liu, Wu, et al., 2017). This value is much lower than that observed in rural areas (Pajunoja et al., 2016) and rainforests (Bateman, Gong, et al., 2015), where particles are predominantly organic. These findings indicate that the presence of inorganic compounds can influence the phase state of aerosol particles.

Urban aerosol particles consist of a large proportion of inorganic compounds, and they frequently internally mix with organic compounds in the atmosphere (Murphy et al., 2006). In Asian cities like Beijing and Seoul, the average mass fraction of inorganic compounds in PM_1 during winter was about 61% and 73%, respectively (Kim et al., 2022). In Los Angeles, particles consisted of an average of 69% inorganic compounds in June, according to the annual report of the US Air Quality Research Center (https://aqrc.ucdavis.edu/). In Europe, the mass fraction of inorganic compounds in PM_1 and fog water was ~50% (Decesari et al., 2014) and 86% (Giulianelli et al., 2014), respectively, in Po Valley, Italy. Global control measures targeting SO_2 emissions to mitigate acid rain have led to a decline in sulfate in fine particles (Hoesly et al., 2018). However, the reduction in NO_x emissions has been less significant. Consequently, nitrate has replaced sulfate as the dominant inorganic component in many cities (Lu et al., 2019). As mentioned earlier, the presence of inorganic compounds has a prominent influence on the aerosol phase state. However, the characteristics of the phase state of urban aerosol particles with abundant inorganic compounds, particularly nitrate-dominated particles, remain largely unknown.

Herein, the effects of inorganic compounds, particularly nitrate, on the phase state of urban aerosol particles were investigated. Rebound behavior measurements were conducted on both laboratory-generated mixtures and regenerated ambient particles from water-extracted filters collected in the field. Results demonstrated that an increased mass fraction of inorganic compounds allowed urban aerosol particles to exist in a liquid state at lower RH levels due to the increased moisture content. Furthermore, with ~50% nitrate mass fraction, particles remained non-solid state even at RH levels as low as 20%. These findings suggest that compared to other aerosol particles, kinetic limitation by bulk diffusion in nitrate-dominated particles can be neglected at lower RH, indicating their potential role as key seeds for secondary aerosol formation through multiphase reactions.

2. Materials and Methods

2.1. Sample Preparation

Daily $PM_{2.5}$ samples were collected at the Peking University Atmospheric Environmental Monitoring Station (PKUERS; 39°59′20″N, 116°18′26″E) in Beijing from October to December 2019. The water-soluble fraction of $PM_{2.5}$ was extracted using pure water (Milli-Q Gradient; 25°C; 18.2 MΩ). Afterward, the solution was atomized into particles, referred to as regenerated ambient particles, using an aerosol atomizer (Model 3076, TSI Inc.).

Inorganic–organic mixtures with different OIRs (the mass ratios of organic to inorganic compounds, detailed values were shown in Table S1 in Supporting Information S1) were prepared using tartaric acid (TA; Adamas, China), which is a common water-soluble low-molecular organic acid (Sato et al., 2021), NH_4NO_3 (Meryer, China), and $(NH_4)_2SO_4$ (Meilunbio, China), which are two of the most abundant inorganic species in the atmosphere (Li et al., 2021). The mixed solution was then nebulized into particles.

Additionally, long-term daily $PM_{2.5}$ samples were collected in Beijing from January to March each year between 2015 and 2020 using a Partisol-plus2025 continuous sampler (R&P, USA) and Teflon filters (16.7 L/min; 47 mm; Whatman, USA) and Quartz filters (16.7 L/min; 47 mm; Whatman, USA). The Teflon filter samples were extracted with pure water and nebulized into particles as well.

The rebound fraction of all the particle samples was determined using a three-arm impactor (introduced in Section 2.2). The chemical composition of regenerated ambient particles was measured by an aerodyne time-of-flight aerosol mass spectrometer. The long-term daily $PM_{2.5}$ samples were analyzed using an ion-chromatograph (IC; DIONEX ICS2000/ICS2500) to determine inorganic anions, and a portion of 1.45 cm^2 was punched from each quartz filter and used to determine organic carbon (OC) with a Sunset OC/EC (elemental carbon) analyzer using the NIOSH method. Organic compounds were estimated by multiplying OC by 1.6 (Xing et al., 2013). Figure S1 in Supporting Information S1 shows the flowchart illustrating aerosol generation and measurements and Table S2 in Supporting Information S1 summarizes the complete data set used in this study.

2.2. Particle Rebound Measurement

The three-arm impactor used here was described in detail in our previous studies (Bateman et al., 2013; Liu, Wu, et al., 2017). In summary, the instrument consisted of three impactors with different impact plates, and the particle rebound fraction (f), which reflected the phase state of particles, was calculated using Equation 1:

$$f = \frac{N_2 - N_3}{N_1 - N_3}, \tag{1}$$

where N_1, N_2, and N_3 are the total particle population, the population of rebounded particles, and the background particle population, respectively. Particles were considered liquid or solid when the rebound fraction was below 0.1 or above 0.8, respectively (Liu et al., 2021; Pajunoja et al., 2016). Otherwise, they were considered semisolid. During the measurement, a silica gel diffusion drier was installed at the front of the devices to ensure the sampling air was dried to an RH below 30%. Measurements were conducted at room temperature (~25°C), and 200-nm particles were selected for rebound fraction measurement. The three-arm impactor was operated in "scan mode," where the RH in the system increased from 5% to 85% in increments of RH = 5%. The "scan mode" generated curves of particle rebound fraction versus RH (Figure S2 in Supporting Information S1). The liquid phase–transition threshold RH ($RH_{threshold}$), at which particles transition from solid/semisolid to a liquid state, corresponding to $f = 0.1$, was determined from the sigmoid-fitting function of the curve. The three-arm impactor was calibrated using standard $(NH_4)_2SO_4$ particles before and after the experiments. Further details can be found in Supporting Information S1.

2.3. Aerosol Liquid Water Content Calculation

The normalized ALWC (hereafter abbreviated as ALWC) was calculated using Equation 2 as follows:

$$\text{ALWC} = \frac{m_{w,\text{inorg}} + m_{w,\text{org}}}{m_p}, \tag{2}$$

where $m_{w,\text{inorg}}$ and $m_{w,\text{org}}$ are the mass concentration of liquid water taken up by inorganic compounds and organic compounds, respectively. The total liquid water content is then normalized by the mass concentration of dry particles (m_p) to enable comparison between different pollution levels. The liquid water taken up by inorganic compounds (NH_4^+, NO_3^-, Cl^-, and SO_4^{2-}) was calculated using the ISORROPIA-II model, and the liquid water contributed by organic compounds was calculated using Eq. [3] (Nguyen et al., 2015):

$$m_{w,\text{org}} = \frac{m_{\text{org}}}{\rho_{\text{org}}} \times \kappa_{\text{org}} \times \frac{\text{RH}}{1 - \text{RH}}, \tag{3}$$

where m_{org} is the mass (μg/m^3) of organic materials, and κ_{org} is the average effective hygroscopicity parameter of organic material. For this study, κ_{org} and ρ_{org} were assumed to be 0.1 (Kuang et al., 2020) and 1 g/cm^3

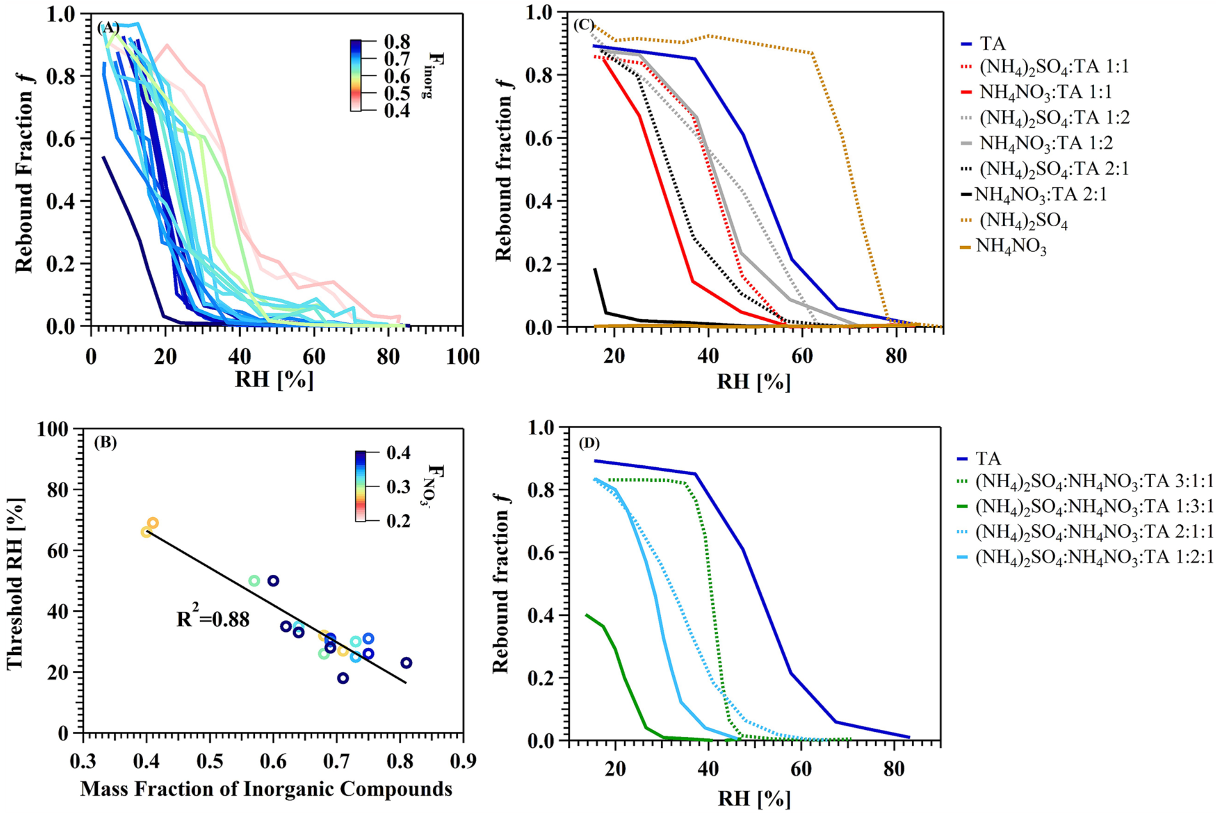

Figure 1. (a) Rebound fraction (f) of regenerated ambient particles (the color of the curves represents the mass fraction of inorganic compounds; F_{inorg}) as a function of relative humidity (RH). (b) Liquid–phase–transition threshold RH ($RH_{threshold}$) of regenerated ambient particles as a function of F_{inorg}. The color of the circles represents the mass fraction of NO_3^- ($F_{NO_3^-}$). (c) Rebound fraction of $(NH_4)_2SO_4$–tartaric acid (TA), NH_4NO_3–TA mixtures, and pure TA, $(NH_4)_2SO_4$, and NH_4NO_3 particles as a function of RH. (d) Rebound fraction of $(NH_4)_2SO_4$–NH_4NO_3–TA mixtures as a function of RH.

(Carrico et al., 2010), respectively. One should note that the calculation of aerosol liquid water followed the Zdanovsky-Stokes-Robinson (ZSR) mixing rule (Robinson et al., 1970), which does not consider the effect of particle morphology.

For regenerated ambient particles and long-term $PM_{2.5}$ samples collected between 2015 and 2020, the ALWC was calculated based on the measured mass concentration of each chemical component, using the same RH values as during the rebound measurements. The liquid phase–transition threshold ALWC ($ALWC_{threshold}$), at which particles exist in a liquid state (indicated by $f = 0.1$), was derived from the sigmoid fitting function of the curve of rebound fraction versus ALWC (Figure S3 in Supporting Information S1). However, for laboratory-generated mixtures, a fixed total particle mass concentration was set to obtain the mass concentration of each inorganic/organic compound based on the OIRs during the ALWC calculation, and the RH was set from 10% to 90% in increments of RH = 10%. Since ALWC represents the mass concentration ratio of aerosol liquid water to dry particles, the ALWC of laboratory-generated mixtures should not be affected by their total mass concentrations.

3. Results and Discussion

3.1. Dependency of Particle Phase State on Inorganic Fractions

Figure 1a shows the rebound fraction of regenerated ambient particles as a function of RH. Each curve represents a daily $PM_{2.5}$ sample and is color-coded based on the dry mass fraction of NH_4^+, NO_3^-, SO_4^{2-}, and Cl^- in dry PM_1 (F_{inorg}). The RH values at which the particle rebound fraction decreased from 0.8 to below 0.1, indicating a phase transition from solid to liquid state, ranged from ~5% to 85%. As F_{inorg} increased from 0.42 to 0.81, the curve of rebound fraction gradually shifted to the left, indicating that the rebound fraction was lower with higher F_{inorg} at the same RH, and the increment of F_{inorg} made urban aerosol less viscous. Moreover, according to the curve on the leftmost side of Figure 1a, which presents particles with F_{inorg} higher than 0.8 and a dry mass fraction of NO_3^- in total dry mass of particles ($F_{NO_3^-}$) as high as 0.53, the rebound fraction was 0.54 even when the RH was below 5%. This implies that a large proportion of nitrate causes particles to remain non-solid under dry conditions.

Figure 1b shows the dependency of the $RH_{threshold}$ (corresponding to $f = 0.1$) of regenerated ambient particles on F_{inorg}. The $RH_{threshold}$ decreased from ~55% to 30% as F_{inorg} increased from ~0.4 to 0.7. The coefficient of determination (R^2) between $RH_{threshold}$ and F_{inorg} was 0.88, indicating a strong linear relationship. The $RH_{threshold}$, derived from our viscosity measurement (poke-and-flow method) of particles in Beijing and Seoul (Song et al., 2022), is depicted in Figure S4 in Supporting Information S1. Despite demonstrating different $RH_{threshold}$ values (discussed in Supporting Information S1), it shared a consistent decreasing trend with an increase in F_{inorg}, thereby exhibiting a clear linear correlation. This linear variation can be explained by the fact that aerosol liquid water primarily determines particle phase state, and the moisture absorbed by inorganic compounds greatly contributes to the water content in particulate matters, as discussed in Section 3.2. Furthermore, when F_{inorg} was the same, particles with higher $F_{NO_3^-}$ exhibited even lower $RH_{threshold}$ values. For example, when F_{inorg} was 0.72, the $RH_{threshold}$ was ~18% for particles in Beijing with $F_{NO_3^-} = 0.44$, whereas $RH_{threshold}$ was 27% for particles with $F_{NO_3^-} = 0.18$. This finding aligns with the results obtained from our field observation conducted in 2018 in Taizhou, China (Liu et al., 2021). As presented in Figure S5 in Supporting Information S1, the $RH_{threshold}$ of atmospheric aerosol particles decreased from approximately 79% to 47% as $F_{NO_3^-}$ increased from 0.05–0.1 to 0.35–0.4. Additionally, Sun et al. (2018) found that an increase in NH_4NO_3 content led to the occurrence of aqueous aerosol particles at lower RH. Therefore, nitrate has a greater impact on the particle phase state compared to other inorganic components.

Figure 1c shows the rebound fraction of $(NH_4)_2SO_4$–TA, NH_4NO_3–TA mixtures, and pure TA, $(NH_4)_2SO_4$, and NH_4NO_3 particles as a function of RH. For $(NH_4)_2SO_4$ and NH_4NO_3 particles, $(NH_4)_2SO_4$ particles transitioned into a liquid state ($f < 0.1$) only when the RH exceeded 78% due to deliquescence, while NH_4NO_3 remained in a liquid state even at RH below 20%. These results are consistent with the findings of Li et al. (2016). For TA, as the RH spanned from ~15% to 85%, the rebound fraction decreased from ~0.89 to 0.01. However, the rebound fraction for inorganic–organic mixtures was lower than that for TA at the same RH. For example, at an RH of ~50%, the rebound fraction for TA and $(NH_4)_2SO_4$–TA with OIRs of 1:2, 1:1, and 2:1 were ~0.51, 0.35, 0.11, and 0.08, respectively. The gradual decrease in rebound fraction with increasing OIRs is consistent with the results of other studies (Jeong et al., 2022; Lilek & Zuend, 2022; Marsh et al., 2018; Power et al., 2013; Song et al., 2021; Sun et al., 2018). Based on the rebound fraction, particles with no inorganic compounds and with inorganic compounds having OIRs of 1:2, 1:1, and 2:1 transformed into a liquid phase at RH values of ~65%, 60%, 51%, and 47%, respectively. The results in Figure 1c also suggest that when F_{inorg} is the same, the rebound fraction of NH_4NO_3–TA particles is lower than that of $(NH_4)_2SO_4$–TA particles at the same RH. With an OIR of 1:1, the rebound fraction of $(NH_4)_2SO_4$–TA particles was ~0.41 higher than that of NH_4NO_3–TA particles at an RH of ~40%, and the rebound fraction corresponded to a liquid state for RH > ~51% ($(NH_4)_2SO_4$–TA) and RH > ~42% (NH_4NO_3–TA). Furthermore, for nitrate-rich NH_4NO_3–TA particles (OIR = 2:1), their rebound fraction remained below 0.8 even at RH values below 20%, implying that they were in a non-solid state rather than a solid state at low RH.

Figure 1d shows the particle rebound fraction (f) versus RH for ternary mixed particles. Similar to the results of binary mixtures, the rebound fraction of inorganic–organic mixtures was lower than that of TA at the same RH, and the rebound fraction of NH_4NO_3-dominated particles was lower than that of $(NH_4)_2SO_4$-dominated particles. The $RH_{threshold}$ was ~65% for TA particles, ~44% for an OIR of 3:1:1 ($(NH_4)_2SO_4$: NH_4NO_3: TA), and ~25% for an OIR of 1:3:1. When the OIR was 1:3:1, the ternary mixed particles were in a non-solid state even under extremely dry conditions, such as an RH below 20%. The results obtained from laboratory-generated mixtures were consistent with those from regenerated ambient particles, indicating that inorganic compounds can decrease the particle rebound fraction, with nitrate having a greater effect on particle phase state than sulfate.

3.2. Role of Aerosol Liquid Water on Particle Phase State

The effect of inorganic compounds on the phase state of inorganic–organic mixed aerosol particles was likely due to the increase in liquid water content with an increasing mass fraction of inorganic compounds at a given RH. This is because water, acting as a plasticizer, plays a crucial role in determining particle phase state (Koop et al., 2011). Figure 2a shows the rebound fraction and the frequency of rebound fraction below 0.1 for regenerated

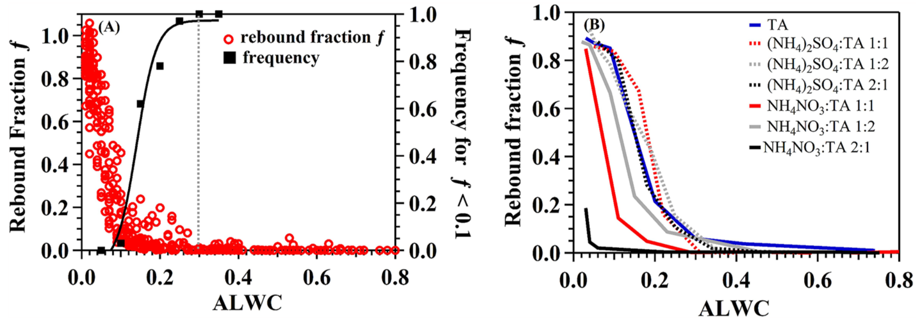

Figure 2. (a) Rebound fraction (f) and frequency for f below 0.1 of regenerated ambient particles as a function of aerosol liquid water content (ALWC). The black line represents the sigmoid-fitting results of the frequency. (b) Rebound fraction of laboratory-generated $(NH_4)_2SO_4$–NH_4NO_3–TA ternary mixed particles as a function of ALWC.

ambient particles as a function of ALWC. The frequency indicates the proportion of particles with a rebound fraction below 0.1 among all particles at a specific ALWC (specific values are provided in Table S3 in Supporting Information S1). When ALWC was below 0.1, the particle rebound fraction decreased rapidly with increasing ALWC. In the ALWC range of 0.1–0.3, the decreasing trend in particle rebound fraction with increasing ALWC became slower, but there was an obvious increase in the frequency of particles with a rebound fraction below 0.1. When ALWC was above 0.3, the frequency equaled 1, suggesting that all particles existed in a liquid state under these conditions. Therefore, the moisture content in urban aerosol particles governs their transition from a solid/semisolid to a liquid phase. Generally, the hygroscopicity parameter (κ) for SOAs is ∼0.1 on average (Kuang et al., 2020), while it is above 0.5 for common inorganic compounds in ambient particles (Carrico et al., 2010). Inorganic compounds tend to absorb more water than organic compounds under the same environmental conditions. Thus, the presence of inorganic compounds allows particles to absorb enough water at lower RH, leading to their transformation into a liquid state. As a result, inorganic compounds play a crucial role in the liquid phase transition of particles.

The influence of NH_4NO_3 is more pronounced than that of $(NH_4)_2SO_4$ likely due to two factors. First, NH_4NO_3 has a higher κ value (derived from cloud condensation nuclei) of 0.67 compared to $(NH_4)_2SO_4$ with a value of 0.61 (Petters & Kreidenweis, 2007). Second, NH_4NO_3 particles are in a “liquid state,” which allows them to exist in a liquid state at lower ALWC. Figure 1c and Li et al. (2016) demonstrated that the rebound fraction of $(NH_4)_2SO_4$ fell below 0.1 only when RH reached 78%. However, the rebound fraction of NH_4NO_3 particles remained lower than 0.1, indicating that NH_4NO_3 particles are always in a liquid state. This discrepancy can be explained by the fact that efflorescence does not occur in NH_4NO_3 particles (Lightstone et al., 2000), making them more likely to exist in a liquid state than other inorganic particles (Sun et al., 2018). Figure 2b shows the rebound fraction of TA, NH_4NO_3–TA, and $(NH_4)_2SO_4$–TA particles as a function of ALWC. For TA, $(NH_4)_2SO_4$–TA, and NH_4NO_3–TA mixtures with an OIR of 1:2, particles transformed into a liquid state when ALWC ranged from 0.22 to 0.28. However, NH_4NO_3–TA mixed particles with OIR of 1:1 and 2:1 had transformed into a liquid state when ALWC were ∼0.14 and 0.04, respectively. This demonstrates that the abundant presence of nitrate can result in a lower $RH_{threshold}$.

3.3. Atmospheric Implications and Conclusion

The above discussion confirms that inorganic components, particularly nitrates, can decrease the $RH_{threshold}$, and facilitate the existence of particles in the liquid state. To further analyze the influences of inorganic compounds on the phase state of urban aerosol particles, we focus on Beijing, the capital city of China, and utilize long-term observation of $PM_{2.5}$ chemical compositions. Due to stringent emission controls, the particle chemical composition in Beijing has undergone significant changes in recent years (Huang et al., 2021; Lei et al., 2021; Li et al., 2021; Xiao et al., 2021). The upline of Figure 3 shows the mass fraction of NO_3^-, SO_4^{2-}, NH_4^+, Cl^-, and organic compounds in $PM_{2.5}$ from 2015 to 2020 under different air pollution levels. The air pollution levels are classified as follows: clean (average daily $PM_{2.5}$ < 35 μg/m^3), moderate polluted (average daily $PM_{2.5}$ between 35 and 75 μg/m^3), and heavy polluted (average daily $PM_{2.5}$ ≥ 75 μg/m^3). The total mass fraction of NH_4^+, NO_3^-, SO_4^{2-}, and Cl^- in $PM_{2.5}$ (F_{inorg}) has increased since 2018. During clean and heavy-polluted days, F_{inorg} increased

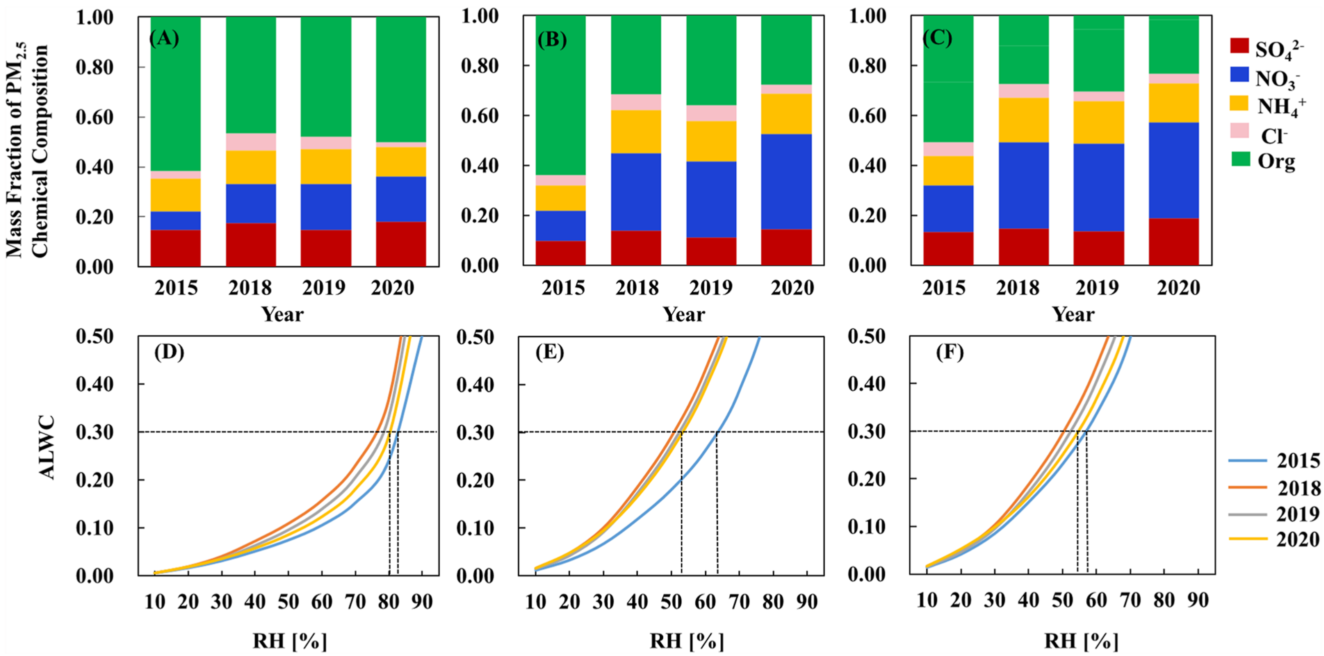

Figure 3. Mass fraction of chemical components in $PM_{2.5}$ (upside panel) and the aerosol liquid water content (ALWC) as a function of relative humidity (RH) (downline) during clean ((a) and (d)), light polluted ((b) and (e)), and polluted ((c) and (f)) days from 2015 to 2020 in the Winter in Beijing.

from 38% and 49% in 2015 to 50% and 77% in 2020, respectively. The most substantial increase in F_{inorg} occurred during moderate-polluted days, rising from 36% in 2015 to 72% in 2020. Additionally, NO_3^- has become the dominant inorganic compound since 2018, replacing SO_4^{2-}. The average $F_{NO_3^-}$ was 12% in 2015, increasing to 33% from 2018 to 2020.

The significant enhancement of F_{inorg} inevitably resulted in higher ALWC at a specific RH. Figures 3d–3f shows the calculated ALWC of $PM_{2.5}$ from 2015 to 2020 as a function of RH under different air pollution levels. When RH is fixed, notable increases in ALWC after 2018 can be observed. The increment of ALWC (Δ_{ALWC}) at a specific RH from 2015 to 2020 was most prominent during moderate-polluted days. For example, at an RH of 50%, the Δ_{ALWC} during clean, moderate-polluted, and heavy-polluted days were ~0.02, 0.08, and 0.02, respectively. This can be attributed to the highest increase in F_{inorg} during the moderate-polluted days, as discussed above.

Based on the results from Figure 2a, ALWC = 0.3 was adopted as the $ALWC_{threshold}$, representing the point at which all particles can exist in the liquid state. The corresponding RH value of the specific aerosol particles is regarded as their $RH_{threshold}$. Consequently, the $RH_{threshold}$ can be derived by polynomial function fitting of the curve in Figures 3d–3f (Figure S6 in Supporting Information S1), which shows the variation of ALWC as a function of RH. The results indicate that the $RH_{threshold}$ tends to decrease from 2018, and the maximum reduction in the $RH_{threshold}$ (Δ_{RH}) for particles from clean to heavy-polluted days was ~2%, 11%, and 2%, respectively. Consistent with Δ_{ALWC}, the highest Δ_{RH}, ranging from ~64% to 53%, was observed during the moderate-polluted days. Besides, since $F_{NO_3^-}$ has notably increased and NO_3^- replaced SO_4^{2-} as the primary inorganic component, Δ_{RH} might exceed 11%. These findings demonstrate that urban aerosol particles in Beijing during winter can transform into a liquid state under drier conditions during air pollution episodes. It is important to note that these results were obtained under the assumption of room temperature, and the effect of temperature on particle phase state was not considered. Additionally, it should be acknowledged that nitrate salts in ambient particles can exist not only as NH_4NO_3 but also as $NaNO_3$, $Ca(NO_3)_2$, etc. However, studies have shown that water-soluble metal ions are minor components in fine particles (Huang et al., 2016; Li et al., 2013; Liu, Xie, et al., 2017; Zhang et al., 2011). Therefore, nitrates are assumed to primarily exist as NH_4NO_3 in this study. Moreover, given that the $RH_{threshold}$ derived here was based on the water-soluble components of the filter samples, non-water soluble components such as certain organic compounds, black carbon, and mineral compounds were not incorporated. Therefore, the $RH_{threshold}$ might be underestimated for atmospheric aerosol particles.

According to the Stokes–Einstein equation, the kinetic limitations of molecule diffusion in the particle phase were expected to diminish at lower RH levels due to the adoption of a liquid state by aerosol particles under drier conditions over the years. To quantitatively analyze this phenomenon, the bulk diffusion coefficient of dioctyl-phthalate (DOP; $D_{f,\,DOP}$) was used as an example. Assuming a viscosity of 10^{-2}, 10^{5}, and 10^{12} Pa s for the liquid, semisolid, and solid state, respectively. In 2015, at an RH of 55%, particles were in the solid state, and the $D_{f,\,DOP}$ was $\sim 10^{-28}$ cm^2/s based on the Stokes–Einstein equation (see Supporting Information S1). However, in 2020, particles were in the liquid state at the same RH and $D_{f,\,DOP}$ correspondingly increased to $\sim 10^{-14}$ cm^2/s. Furthermore, with the increase in $F_{NO_3^-}$, particles can now even exist in a non-solid state at RH < 20%, resulting in a $D_{f,\,DOP}$ above $\sim 10^{-21}$ cm^2/s under such dry conditions. Although the results of the Stokes–Einstein equation calculated at high viscosity may not be accurate, it can be concluded that the change in the chemical composition of urban aerosol particles has significantly enhanced the diffusion coefficients of molecules by several orders of magnitude under drier conditions. Consequently, during the moderate-polluted period, when particles are predominantly nitrate-dominated, the switch to a liquid state occurs even at lower RH levels, facilitating the mass transfer of reactive molecules and promoting the growth and aging of secondary aerosol particles. Additionally, the positive feedback loop between aerosol liquid water and inorganic compounds, which is well documented in previous studies (Chen et al., 2022; Liu, Wu, et al., 2017; Wang et al., 2020; Wu et al., 2018), is more likely to be initiated under these conditions.

For the first time, we have emphasized that the increase in F_{inorg}, especially $F_{NO_3^-}$, in recent years has accelerated bulk–phase diffusion and multiphase chemistry under drier conditions from the perspective of the particle phase state. Our findings highlight the importance of considering the decrease in $RH_{threshold}$ resulting from the enhancement of inorganic compounds to better understand the haze formation mechanisms. Apart from Beijing, noticeable increases in F_{inorg} or $F_{NO_3^-}$ have occurred in many urban cities globally in recent decades. The chemical composition of urban aerosol particles was compiled from various countries (Figure S7 in Supporting Information S1), and it was observed that inorganic compounds can account for 20%–90% of fine particles, while nitrate can account for 2%–66%. In cities where a high proportion of inorganic compounds, particularly particulate nitrate, is present, aerosol particles can exist in the liquid state under drier conditions, such as RH of ∼50%. Therefore, changes in the particle phase state characteristics driven by their chemical properties should also be considered to accurately assess the mass-transfer processes between the gas and particle phases in these cities.

Data Availability Statement

The data sets associated with this manuscript are available at Liu et al. (2023).

Acknowledgments
This work is supported by the following projects: National Natural Science Foundation of China (Grants 42205102 and 91844301) and the Fine Particle Research Initiative in East Asia Considering National Differences (FRIEND) Project (NRF-2020M3G1A1114548).

References

Bateman, A. P., Belassein, H., & Martin, S. T. (2013). Impactor apparatus for the study of particle rebound: Relative humidity and capillary forces. *Aerosol Science and Technology*, *48*(1), 42–52. https://doi.org/10.1080/02786826.2013.853866

Bateman, A. P., Bertram, A. K., & Martin, S. T. (2015). Hygroscopic influence on the semisolid-to-liquid transition of secondary organic materials. *The Journal of Physical Chemistry A*, *119*(19), 4386–4395. https://doi.org/10.1021/jp508521c

Bateman, A. P., Gong, Z., Liu, P., Sato, B., Cirino, G., Zhang, Y., et al. (2015). Sub-micrometre particulate matter is primarily in liquid form over Amazon rainforest. *Nature Geoscience*, *9*(1), 34–37. https://doi.org/10.1038/ngeo2599

Carrico, C. M., Petters, M. D., Kreidenweis, S. M., Sullivan, A. P., McMeeking, G. R., Levin, E. J. T., et al. (2010). Water uptake and chemical composition of fresh aerosols generated in open burning of biomass. *Atmospheric Chemistry and Physics*, *10*(11), 5165–5178. https://doi.org/10.5194/acp-10-5165-2010

Chen, Y., Wang, Y., Nenes, A., Wild, O., Song, S., Hu, D., et al. (2022). Ammonium chloride associated aerosol liquid water enhances haze in Delhi, India. *Environmental Science & Technology*, *56*(11), 7163–7173. https://doi.org/10.1021/acs.est.2c00650

Davies, J. F., & Wilson, K. R. (2015). Nanoscale interfacial gradients formed by the reactive uptake of OH radicals onto viscous aerosol surfaces. *Chemical Science*, *6*(12), 7020–7027. https://doi.org/10.1039/c5sc02326b

Decesari, S., Allan, J., Plass-Duelmer, C., Williams, B. J., Paglione, M., Facchini, M. C., et al. (2014). Measurements of the aerosol chemical composition and mixing state in the Po Valley using multiple spectroscopic techniques. *Atmospheric Chemistry and Physics*, *14*(22), 12109–12132. https://doi.org/10.5194/acp-14-12109-2014

DeRieux, W. S. W., Li, Y., Lin, P., Laskin, J., Laskin, A., Bertram, A. K., et al. (2018). Predicting the glass transition temperature and viscosity of secondary organic material using molecular composition. *Atmospheric Chemistry and Physics*, *18*(9), 6331–6351. https://doi.org/10.5194/acp-18-6331-2018

Giulianelli, L., Gilardoni, S., Tarozzi, L., Rinaldi, M., Decesari, S., Carbone, C., et al. (2014). Fog occurrence and chemical composition in the Po valley over the last twenty years. *Atmospheric Environment*, *98*, 394–401. https://doi.org/10.1016/j.atmosenv.2014.08.080

Grayson, J. W., Evoy, E., Song, M., Chu, Y., Maclean, A., Nguyen, A., et al. (2017). The effect of hydroxyl functional groups and molar mass on the viscosity of non-crystalline organic and organic–water particles. *Atmospheric Chemistry and Physics*, *17*(13), 8509–8524. https://doi.org/10.5194/acp-17-8509-2017

Hoesly, R. M., Smith, S. J., Feng, L., Klimont, Z., Janssens-Maenhout, G., Pitkanen, T., et al. (2018). Historical (1750–2014) anthropogenic emissions of reactive gases and aerosols from the Community Emissions Data System (CEDS). *Geoscientific Model Development*, *11*(1), 369–408. https://doi.org/10.5194/gmd-11-369-2018

Hosny, N. A., Fitzgerald, C., Vyšniauskas, A., Athanasiadis, A., Berkemeier, T., Uygur, N., et al. (2016). Direct imaging of changes in aerosol particle viscosity upon hydration and chemical aging. *Chemical Science*, *7*(2), 1357–1367. https://doi.org/10.1039/c5sc02959g

Huang, X., Liu, Z., Zhang, J., Wen, T., Ji, D., & Wang, Y. (2016). Seasonal variation and secondary formation of size-segregated aerosol water-soluble inorganic ions during pollution episodes in Beijing. *Atmospheric Research*, *168*, 70–79. https://doi.org/10.1016/j.atmosres.2015.08.021

Huang, X., Tang, G., Zhang, J., Liu, B., Liu, C., Zhang, J., et al. (2021). Characteristics of PM2.5 pollution in Beijing after the improvement of air quality. *Journal of Environmental Sciences*, *100*, 1–10. https://doi.org/10.1016/j.jes.2020.06.004

Jeong, R., Lilek, J., Zuend, A., Xu, R., Chan, M. N., Kim, D., et al. (2022). Viscosity and physical state of sucrose mixed with ammonium sulfate droplets. *Atmospheric Chemistry and Physics*, *2022*, 1–21. https://doi.org/10.5194/acp-2022-74

Kaluarachchi, C. P., Or, V. W., Lan, Y., Madawala, C. K., Hasenecz, E. S., Crocker, D. R., et al. (2022). Size-dependent morphology, composition, phase state, and water uptake of nascent submicrometer sea spray aerosols during a phytoplankton bloom. *ACS Earth and Space Chemistry*, *6*(1), 116–130. https://doi.org/10.1021/acsearthspacechem.1c00306

Kim, N. K., Kim, Y. P., Ghim, Y. S., Song, M. J., Kim, C. H., Jang, K. S., et al. (2022). Spatial distribution of PM2.5 chemical components during winter at five sites in Northeast Asia: High temporal resolution measurement study. *Atmospheric Environment*, *290*, 119359. https://doi.org/10.1016/j.atmosenv.2022.119359

Koop, T., Bookhold, J., Shiraiwa, M., & Pöschl, U. (2011). Glass transition and phase state of organic compounds: Dependency on molecular properties and implications for secondary organic aerosols in the atmosphere. *Physical Chemistry Chemical Physics*, *13*(43), 19238. https://doi.org/10.1039/c1cp22617g

Kuang, Y., Xu, W., Tao, J., Ma, N., Zhao, C., & Shao, M. (2020). A review on laboratory studies and field measurements of atmospheric organic aerosol hygroscopicity and its parameterization based on oxidation levels. *Current Pollution Reports*, *6*(4), 410–424. https://doi.org/10.1007/s40726-020-00164-2

Kucinski, T. M., Dawson, J. N., & Freedman, M. A. (2019). Size-dependent liquid–liquid phase separation in atmospherically relevant complex systems. *Journal of Physical Chemistry Letters*, *10*(21), 6915–6920. https://doi.org/10.1021/acs.jpclett.9b02532

Kuwata, M., & Martin, S. T. (2012). Phase of atmospheric secondary organic material affects its reactivity. *Proceedings of the National Academy of Sciences*, *109*(43), 17354–17359. https://doi.org/10.1073/pnas.1209071109

Lei, L., Zhou, W., Chen, C., He, Y., Li, Z., Sun, J., et al. (2021). Long-term characterization of aerosol chemistry in cold season from 2013 to 2020 in Beijing, China. *Environmental Pollution*, *268*, 115952. https://doi.org/10.1016/j.envpol.2020.115952

Li, J., Gao, W., Cao, L., Xiao, Y., Zhang, Y., Zhao, S., et al. (2021). Significant changes in autumn and winter aerosol composition and sources in Beijing from 2012 to 2018: Effects of clean air actions. *Environmental Pollution*, *268*, 115855. https://doi.org/10.1016/j.envpol.2020.115855

Li, X., Wang, L., Ji, D., Wen, T., Pan, Y., Sun, Y., & Wang, Y. (2013). Characterization of the size-segregated water-soluble inorganic ions in the Jing-Jin-Ji urban agglomeration: Spatial/temporal variability, size distribution and sources. *Atmospheric Environment*, *77*, 250–259. https://doi.org/10.1016/j.atmosenv.2013.03.042

Li, Y., Day, D. A., Stark, H., Jimenez, J. L., & Shiraiwa, M. (2020). Predictions of the glass transition temperature and viscosity of organic aerosols from volatility distributions. *Atmospheric Chemistry and Physics*, *20*(13), 8103–8122. https://doi.org/10.5194/acp-20-8103-2020

Li, Y. J., Liu, P. F., Bergoend, C., Bateman, A. P., & Martin, S. T. (2016). Rebounding hygroscopic inorganic aerosol particles: Liquids, gels, and hydrates. *Aerosol Science and Technology*, *51*(3), 388–396. https://doi.org/10.1080/02786826.2016.1263384

Lightstone, J. M., Onasch, T. B., Imre, D., & Oatis, S. (2000). Deliquescence, efflorescence, and water activity in ammonium nitrate and mixed ammonium nitrate/succinic acid microparticles. *The Journal of Physical Chemistry A*, *104*(41), 9337–9346. https://doi.org/10.1021/jp002137h

Lilek, J., & Zuend, A. (2022). A predictive viscosity model for aqueous electrolytes and mixed organic–inorganic aerosol phases. *Atmospheric Chemistry and Physics*, *22*(5), 3203–3233. https://doi.org/10.5194/acp-22-3203-2022

Liu, Y., Meng, X., Wu, Z., Huang, D., Wang, H., Chen, J., et al. (2021). The particle phase state during the biomass burning events. *The Science of the Total Environment*, *792*, 148035. https://doi.org/10.1016/j.scitotenv.2021.148035

Liu, Y., Wu, Z., Qiu, Y., Tian, P., Liu, Q., Chen, Y., et al. (2023). Enhanced nitrate fraction: Enabling urban aerosols particles to remain in a liquid state at reduced relative humidity [Dataset]. Zenodo. https://doi.org/10.5281/zenodo.8188863

Liu, Y., Wu, Z., Wang, Y., Xiao, Y., Gu, F., Zheng, J., et al. (2017). Submicrometer particles are in the liquid state during heavy haze episodes in the urban atmosphere of Beijing, China. *Environmental Science and Technology Letters*, *4*(10), 427–432. https://doi.org/10.1021/acs.estlett.7b00352

Liu, Z., Xie, Y., Hu, B., Wen, T., Xin, J., Li, X., & Wang, Y. (2017). Size-resolved aerosol water-soluble ions during the summer and winter seasons in Beijing: Formation mechanisms of secondary inorganic aerosols. *Chemosphere*, *183*, 119–131. https://doi.org/10.1016/j.chemosphere.2017.05.095

Lu, K., Fuchs, H., Hofzumahaus, A., Tan, Z., Zhang, Y., Zhang, L., et al. (2019). Fast photochemistry in wintertime haze: Consequences for pollution mitigation strategies. *Environmental Science and Technology*, *53*(18), 10676–10684. https://doi.org/10.1021/acs.est.9b02422

Marsh, A., Petters, S. S., Rothfuss, N. E., Rovelli, G., Song, Y. C., Reid, J. P., & Petters, M. D. (2018). Amorphous phase state diagrams and viscosity of ternary aqueous organic/organic and inorganic/organic mixtures. *Physical Chemistry Chemical Physics*, *20*(22), 15086–15097. https://doi.org/10.1039/C8CP00760H

Mu, Q., Shiraiwa, M., Octaviani, M., Ma, N., Ding, A., Su, H., et al. (2018). Temperature effect on phase state and reactivity controls atmospheric multiphase chemistry and transport of PAHs. *Science Advances*, *4*(3), eaap7314. https://doi.org/10.1126/sciadv.aap7314

Murphy, D. M., Cziczo, D. J., Froyd, K. D., Hudson, P. K., Matthew, B. M., Middlebrook, A. M., et al. (2006). Single-particle mass spectrometry of tropospheric aerosol particles. *Journal of Geophysical Research*, *111*(D23). https://doi.org/10.1029/2006JD007340

Nguyen, T. K., Capps, S., & Carlton, A. M. (2015). *Decreasing aerosol water is consistent with OC trends in the Southeast*. U.S.

Pajunoja, A., Hu, W., Leong, Y. J., Taylor, N. F., Miettinen, P., Palm, B. B., et al. (2016). Phase state of ambient aerosol linked with water uptake and chemical aging in the Southeastern US. *Atmospheric Chemistry and Physics*, *16*(17), 1–25. https://doi.org/10.5194/acp-16-11163-2016

Pajunoja, A., Malila, J., Hao, L., Joutsensaari, J., Lehtinen, K. E. J., & Virtanen, A. (2014). Estimating the viscosity range of SOA particles based on their coalescence time. *Aerosol Science and Technology*, *48*(2), i–iv. https://doi.org/10.1080/02786826.2013.870325

Petters, M., & Kreidenweis, S. (2007). A single parameter representation of hygroscopic growth and cloud condensation nucleus activity. *Atmospheric Chemistry and Physics*, *7*(8), 1961–1971. https://doi.org/10.5194/acp-7-1961-2007

Pöschl, U. (2005). Atmospheric aerosols: Composition, transformation, climate and health effects. *Angewandte Chemie International Edition*, *44*(46), 7520–7540. https://doi.org/10.1002/anie.200501122

Power, R. M., Simpson, S. H., Reid, J. P., & Hudson, A. J. (2013). The transition from liquid to solid-like behaviour in ultrahigh viscosity aerosol particles. *Chemical Science*, *4*(6), 2597. https://doi.org/10.1039/c3sc50682g

Reid, J. P., Bertram, A. K., Topping, D. O., Laskin, A., Martin, S. T., Petters, M. D., et al. (2018). The viscosity of atmospherically relevant organic particles. *Nature Communications*, *9*(1), 956. https://doi.org/10.1038/s41467-018-03027-z

Renbaum-Wolff, L., Grayson, J. W., Bateman, A. P., Kuwata, M., Sellier, M., Murray, B. J., et al. (2013). Viscosity of -pinene secondary organic material and implications for particle growth and reactivity. *Proceedings of the National Academy of Sciences*, *110*(20), 8014–8019. https://doi.org/10.1073/pnas.1219548110

Robinson, R. A., Stokes, R. H., & Marsh, K. N. (1970). Activity coefficients in the ternary system: Water + sucrose + sodium chloride. *The Journal of Chemical Thermodynamics*, *2*(5), 745–750. https://doi.org/10.1016/0021-9614(70)90050-9

Rothfuss, N. E., & Petters, M. D. (2017). Influence of functional groups on the viscosity of organic aerosol. *Environmental Science & Technology*, *51*(1), 271–279. https://doi.org/10.1021/acs.est.6b04478

Sato, K., Ikemori, F., Ramasamy, S., Fushimi, A., Kumagai, K., Iijima, A., & Morino, Y. (2021). Four- and five-carbon dicarboxylic acids present in secondary organic aerosol produced from anthropogenic and biogenic volatile organic compounds. *Atmosphere*, *12*(12), 1703. https://doi.org/10.3390/atmos12121703

Saukko, E., Lambe, A. T., Massoli, P., Koop, T., Wright, J. P., Croasdale, D. R., et al. (2012). Humidity-dependent phase state of SOA particles from biogenic and anthropogenic precursors. *Atmospheric Chemistry and Physics*, *12*(16), 7517–7529. https://doi.org/10.5194/acp-12-7517-2012

Shiraiwa, M., Ammann, M., Koop, T., & Poschl, U. (2011). Gas uptake and chemical aging of semisolid organic aerosol particles. *Proceedings of the National Academy of Sciences Unoted states of America*, *108*(27), 11003–11008. https://doi.org/10.1073/pnas.1103045108

Shiraiwa, M., Li, Y., Tsimpidi, A. P., Karydis, V. A., Berkemeier, T., Pandis, S. N., et al. (2017). Global distribution of particle phase state in atmospheric secondary organic aerosols. *Nature Communications*, *8*(1), 15002. https://doi.org/10.1038/ncomms15002

Shiraiwa, M., Pfrang, C., & Pöschl, U. (2010). Kinetic multi-layer model of aerosol surface and bulk chemistry (KM-SUB): The influence of interfacial transport and bulk diffusion on the oxidation of oleic acid by ozone. *Atmospheric Chemistry and Physics*, *10*(8), 3673–3691. https://doi.org/10.5194/acp-10-3673-2010

Song, M., Jeong, R., Kim, D., Qiu, Y., Meng, X., Wu, Z., et al. (2022). Comparison of phase states of PM2.5 over megacities, Seoul and Beijing, and their implications on particle size distribution. *Environmental Science & Technology*, *56*(24), 17581–17590. https://doi.org/10.1021/acs.est.2c06377

Song, M., Liu, P. F., Hanna, S. J., Li, Y. J., Martin, S. T., & Bertram, A. K. (2015). Relative humidity-dependent viscosities of isoprene-derived secondary organic material and atmospheric implications for isoprene-dominant forests. *Atmospheric Chemistry and Physics*, *15*(9), 5145–5159. https://doi.org/10.5194/acp-15-5145-2015

Song, M., Liu, P. F., Hanna, S. J., Zaveri, R. A., Potter, K., You, Y., et al. (2016). Relative humidity-dependent viscosity of secondary organic material from toluene photo-oxidation and possible implications for organic particulate matter over megacities. *Atmospheric Chemistry and Physics*, *16*(14), 8817–8830. https://doi.org/10.5194/acp-16-8817-2016

Song, Y. C., Lilek, J., Lee, J. B., Chan, M. N., Wu, Z., Zuend, A., & Song, M. (2021). Viscosity and phase state of aerosol particles consisting of sucrose mixed with inorganic salts. *Atmospheric Chemistry and Physics*, *21*(13), 10215–10228. https://doi.org/10.5194/acp-21-10215-2021

Sun, J., Liu, L., Xu, L., Wang, Y., Wu, Z., Hu, M., et al. (2018). Key role of nitrate in phase transitions of urban particles: Implications of important reactive surfaces for secondary aerosol formation. *Journal of Geophysical Research: Atmospheres*, *123*(2), 1234–1243. https://doi.org/10.1002/2017JD027264

Tong, Y.-K., Liu, Y., Meng, X., Wang, J., Zhao, D., Wu, Z., & Ye, A. (2022). The relative humidity-dependent viscosity of single quasi aerosol particles and possible implications for atmospheric aerosol chemistry. *Physical Chemistry Chemical Physics*, *24*(17), 10514–10523. https://doi.org/10.1039/D2CP00740A

Wang, Y., Chen, Y., Wu, Z., Shang, D., Bian, Y., Du, Z., et al. (2020). Mutual promotion between aerosol particle liquid water and particulate nitrate enhancement leads to severe nitrate-dominated particulate matter pollution and low visibility. *Atmospheric Chemistry and Physics*, *20*(4), 2161–2175. https://doi.org/10.5194/acp-20-2161-2020

Wu, Z., Wang, Y., Tan, T., Zhu, Y., Li, M., Shang, D., et al. (2018). Aerosol liquid water driven by anthropogenic inorganic salts: Implying its key role in haze formation over the North China Plain. *Environmental Science and Technology Letters*, *5*(3), 160–166. https://doi.org/10.1021/acs.estlett.8b00021

Xiao, Y., Hu, M., Zong, T., Wu, Z., Tan, T., Zhang, Z., et al. (2021). Insights into aqueous-phase and photochemical formation of secondary organic aerosol in the winter of Beijing. *Atmospheric Environment*, *259*, 118535. https://doi.org/10.1016/j.atmosenv.2021.118535

Xing, L., Fu, T. M., Cao, J. J., Lee, S. C., Wang, G. H., Ho, K. F., et al. (2013). Seasonal and spatial variability of the OM/OC mass ratios and high regional correlation between oxalic acid and zinc in Chinese urban organic aerosols. *Atmospheric Chemistry and Physics*, *13*(8), 4307–4318. https://doi.org/10.5194/acp-13-4307-2013

Zhang, T., Cao, J. J., Tie, X. X., Shen, Z. X., Liu, S. X., Ding, H., et al. (2011). Water-soluble ions in atmospheric aerosols measured in Xi'an, China: Seasonal variations and sources. *Atmospheric Research*, *102*(1), 110–119. https://doi.org/10.1016/j.atmosres.2011.06.014

References From the Supporting Information

Chowdhury, M. Z. (2004). Characterization of fine particle air pollution in the Indian Subcontinent.

Fountoukis, C., & Nenes, A. (2007). ISORROPIA II: A computationally efficient thermodynamic equilibrium model for K^+–Ca^{2+}–Mg^{2+}–NH_4^+–Na^+–SO_4^{2-}–NO_3^-–Cl^-–H_2O aerosols. *Atmospheric Chemistry and Physics*, *7*(17), 4639–4659. https://doi.org/10.5194/acp-7-4639-2007

Herrera Murillo, J., Campos Ramos, A., Ángeles García, F., Blanco Jiménez, S., Cárdenas, B., & Mizohata, A. (2012). Chemical composition of PM2.5 particles in Salamanca, Guanajuato Mexico: Source apportionment with receptor models. *Atmospheric Research*, *107*, 31–41. https://doi.org/10.1016/j.atmosres.2011.12.010

Huang, R.-J., Zhang, Y., Bozzetti, C., Ho, K.-F., Cao, J.-J., Han, Y., et al. (2014). High secondary aerosol contribution to particulate pollution during haze events in China. *Nature*, *514*(7521), 218–222. https://doi.org/10.1038/nature13774

Hussein, T., Puustinen, A., Aalto, P. P., Mäkelä, J. M., Hämeri, K., & Kulmala, M. (2004). Urban aerosol number size distributions. *Atmospheric Chemistry and Physics*, *4*(2), 391–411. https://doi.org/10.5194/acp-4-391-2004

Jiang, N., Guo, Y., Wang, Q., Kang, P., Zhang, R., & Tang, X. (2017). Chemical composition characteristics of PM2.5 in three cities in Henan, Central China. *Aerosol and Air Quality Research*, *17*(10), 2367–2380. https://doi.org/10.4209/aaqr.2016.10.0463

Joseph, A. E., Unnikrishnan, S., & Kumar, R. (2012). Chemical characterization and mass closure of fine aerosol for different land use patterns in Mumbai City. *Aerosol and Air Quality Research*, *12*(1), 61–72. https://doi.org/10.4209/aaqr.2011.04.0049

Kong, L., Tan, Q., Feng, M., Qu, Y., An, J., Liu, X., et al. (2020). Investigating the characteristics and source analyses of PM2.5 seasonal variations in Chengdu, Southwest China. *Chemosphere*, *243*, 125267. https://doi.org/10.1016/j.chemosphere.2019.125267

Li, Y. J., Sun, Y., Zhang, Q., Li, X., Li, M., Zhou, Z., & Chan, C. K. (2017). Real-time chemical characterization of atmospheric particulate matter in China: A review. *Atmospheric Environment*, *158*, 270–304. https://doi.org/10.1016/j.atmosenv.2017.02.027

Liu, Y., Wu, Z., Tan, T., Wang, Y., Qin, Y., Zheng, J., et al. (2016). Estimation of the PM2.5 effective hygroscopic parameter and water content based on particle chemical composition: Methodology and case study. *Science China Earth Sciences*, *59*(8), 1683–1691. https://doi.org/10.1007/s11430-016-5313-9

Lowenthal, D. H., Gertler, A. W., & Labib, M. W. (2014). Particulate matter source apportionment in Cairo: Recent measurements and comparison with previous studies. *International journal of Environmental Science and Technology*, *11*(3), 657–670. https://doi.org/10.1007/s13762-013-0272-6

Meng, J. W., Yeung, M. C., Li, Y. J., Lee, B. Y. L., & Chan, C. K. (2014). Size-resolved cloud condensation nuclei (CCN) activity and closure analysis at the HKUST Supersite in Hong Kong. *Atmospheric Chemistry and Physics*, *14*(18), 10267–10282. https://doi.org/10.5194/acp-14-10267-2014

Rodríguez, S., Van Dingenen, R., Putaud, J. P., Dell'Acqua, A., Pey, J., Querol, X., et al. (2007). A study on the relationship between mass concentrations, chemistry and number size distribution of urban fine aerosols in Milan, Barcelona and London. *Atmospheric Chemistry and Physics*, *7*(9), 2217–2232. https://doi.org/10.5194/acp-7-2217-2007

Shiraiwa, M., Pfrang, C., Koop, T., & Pöschl, U. (2012). Kinetic multi-layer model of gas-particle interactions in aerosols and clouds (KM-GAP): Linking condensation, evaporation and chemical reactions of organics, oxidants and water. *Atmospheric Chemistry and Physics*, *12*(5), 2777–2794. https://doi.org/10.5194/acp-12-2777-2012

Souza, D. Z., Vasconcellos, P. C., Lee, H., Aurela, M., Saarnio, K., Teinilä, K., & Hillamo, R. (2014). Composition of PM2.5 and PM10 collected at urban sites in Brazil. *Aerosol and Air Quality Research*, *14*(1), 168–176. https://doi.org/10.4209/aaqr.2013.03.0071

Tefera, W., Kumie, A., Berhane, K., Gilliland, F., Lai, A., Sricharoenvech, P., et al. (2021). Source apportionment of fine organic particulate matter (PM2.5) in Central Addis Ababa, Ethiopia. *International Journal of Environmental Research and Public Health*, *18*(21), 11608. https://doi.org/10.3390/ijerph182111608

Tsai, Y. I., Sopajaree, K., Kuo, S.-C., & Yu, S.-P. (2015). Potential PM2.5 impacts of festival-related burning and other inputs on air quality in an urban area of southern Taiwan. *The Science of the Total Environment*, *527–528*, 65–79. https://doi.org/10.1016/j.scitotenv.2015.04.021

Turap, Y., Talifu, D., Wang, X., Abulizi, A., Maihemuti, M., Tursun, Y., et al. (2019). Temporal distribution and source apportionment of PM2.5 chemical composition in Xinjiang, NW-China. *Atmospheric Research*, *218*, 257–268. https://doi.org/10.1016/j.atmosres.2018.12.010

Villalobos, A. M., Barraza, F., Jorquera, H., & Schauer, J. J. (2015). Chemical speciation and source apportionment of fine particulate matter in Santiago, Chile, 2013. *The Science of the Total Environment*, *512–513*, 133–142. https://doi.org/10.1016/j.scitotenv.2015.01.006

Virtanen, A., Kannosto, J., Kuuluvainen, H., Arffman, A., Joutsensaari, J., Saukko, E., et al. (2011). Bounce behavior of freshly nucleated biogenic secondary organic aerosol particles. *Atmospheric Chemistry and Physics*, *11*(16), 8759–8766. https://doi.org/10.5194/acp-11-8759-2011

Wang, P., Cao, J.-J., Shen, Z.-X., Han, Y.-M., Lee, S.-C., Huang, Y., et al. (2015). Spatial and seasonal variations of PM2.5 mass and species during 2010 in Xi'an, China. *The Science of the Total Environment*, *508*, 477–487. https://doi.org/10.1016/j.scitotenv.2014.11.007

Wang, Y., Chen, J., Wang, Q., Qin, Q., Ye, J., Han, Y., et al. (2019). Increased secondary aerosol contribution and possible processing on polluted winter days in China. *Environment International*, *127*, 78–84. https://doi.org/10.1016/j.envint.2019.03.021[

Wang, Y. C., Huang, R. J., Ni, H. Y., Chen, Y., Wang, Q. Y., Li, G. H., et al. (2017). Chemical composition, sources and secondary processes of aerosols in Baoji city of northwest China. *Atmospheric Environment*, *158*, 128–137. https://doi.org/10.1016/j.atmosenv.2017.03.026

Wu, T., & Boor, B. E. (2021). Urban aerosol size distributions: A global perspective. *Atmospheric Chemistry and Physics*, *21*(11), 8883–8914. https://doi.org/10.5194/acp-21-8883-2021

Xu, J., Song, S., Harrison, R. M., Song, C., Wei, L., Zhang, Q., et al. (2020). An interlaboratory comparison of aerosol inorganic ion measurements by ion chromatography: Implications for aerosol pH estimate. *Atmospheric Measurement Techniques*, *13*(11), 6325–6341. https://doi.org/10.5194/amt-13-6325-2020

Yu, Y., Wang, H., Wang, T., Song, K., Tan, T., Wan, Z., et al. (2021). Elucidating the importance of semi-volatile organic compounds to secondary organic aerosol formation at a regional site during the EXPLORE-YRD campaign. *Atmospheric Environment*, *246*, 118043. https://doi.org/10.1016/j.atmosenv.2020.118043

Zhang, F., Wang, Z.-w., Cheng, H.-r., Lv, X.-p., Gong, W., Wang, X.-m., & Zhang, G. (2015). Seasonal variations and chemical characteristics of PM2.5 in Wuhan, central China. *The Science of the Total Environment*, *518–519*, 97–105. https://doi.org/10.1016/j.scitotenv.2015.02.054

Zhao, Z., Lv, S., Zhang, Y., Zhao, Q., Shen, L., Xu, S., et al. (2019). Characteristics and source apportionment of PM2.5 in Jiaxing, China. *Environmental Science and Pollution Research*, *26*(8), 7497–7511. https://doi.org/10.1007/s11356-019-04205-2